Analysis on corrosion resistant of electrodeposited ternary Co-W-P alloy

[*]B. I. Oladapo[*a], S. A. Zahedi[a], A. O. Awe[b], F. T. Omigbodun[a], V. A. Adebiyi[a]

[a] *School of Engineering and Sustainable Development, De Montfort University, Leicester, UK*
[b] *Department of Petroleum Engineering, Rivers State University, Port Harcourt, Rivers State, Nigeria*

Abstract
The interest in the electrodeposition of tungsten-rich binary and ternary alloys has increased in recent years due to their unique combination of electrical, tribological, electro-erosion and magnetic properties. In this research, a ternary alloy of Cobalt-Tungsten-Phosphorus (Co-W-P) is electrodeposited using an electrolyte bath with a relatively low pH, and complexing agents to stabilize the bath, in order to obtain good quality films that increase the life of the substrate. The effect of current density and pH are explored thoroughly to obtain a Co-W-P ternary alloy resistant to corrosion. Transverse-sectional views of the electrodeposited samples are extracted, and the surface roughness, waviness profile, and Gaussian filter of the films are evaluated. The characterisation of the alloy morphology is investigated by a fluorescence spectroscopy technique and scanning electron microscopy (SEM). It is shown that a current density of 6 mA/cm² and pH of 4.0 are the best running parameters to achieve a corrosion resistant film.

Keywords*:* Co-W-P; Corrosion resistance; Electrodeposition; Factorial design

1. Introduction
The electrodeposition method is widely used in the surface finishing industry to improve surface characteristics. The technique consists of depositing a thin layer of coating onto a substrate [1]. This electroplating method presents significant advantages compared to welding or plasma deposition chemistry techniques, due to the lower processing temperature, better control over the process and thus wider range of composition [2-4]. All coatings mainly aim to provide a barrier to the transport of corrosive species to the substrate [5-6].
The interest in the electrodeposition of tungsten-rich binary and ternary alloys has increased in recent years due to their unique combination of electrical, tribological, electro-erosion and magnetic properties [7]. Tungsten-rich alloys show excellent wear resistance in applications such as valves, dies, cutting tools, gas turbines and jet engines [8-10]. Tungsten metal cannot be electrodeposited in a pure state by aqueous electrolytes themselves, but can be codeposited with transition metals from aqueous solutions. The development of a stable bath with a relatively low pH and complexing agents for stabilisation are critical to obtaining good quality films. Cobalt-Tungsten-Phosphorus (Co-W-P) coating has valuable applications as a thin layer on a copper substrate in microelectronic devices, to prevent oxidation [11]. This film has useful features such as wear and corrosion resistance and high hardness that provide superior and unique properties for use in the sophisticated automobile industry, rockets, space technology and micro and nanosystems [12-14].
There is much research into the co-production of W-P layers on copper substrates by electrodeposition from aqueous solution [15-16]. It is reported that tungsten and phosphorus cannot be electro-deposited individually from aqueous electrolyte. Tungsten and phosphorus should deposit in aqueous solutions containing iron group metals (Fe, Co, Ni), which is referred to as induced co-deposition. Therefore, the effects of dispersion concentration in the electrolytic bath on the stability of the various suspensions, as well as the morphology, chemical composition, antibacterial activity and structural coatings obtained using an electrolytic bath of suspended nanoparticles, are important [17].

The main aim of this research is to improve the corrosion resistance of Co-W-P alloy by testing electrodeposition under various operating conditions of current density and pH. Experimental factorial design is used to select operational conditions, which has many advantages over invariant methods. In this technique, parameters are varied simultaneously instead of being set one-to-one as in classical methods, allowing antagonistic interactions and the synergy involved in the analysed factors to be seen. In this study the response surface methodology (RSM) technique is used to improve and optimise operational parameters. The primary objective of RSM is to determine the optimal conditions of operation of a system or define an operating region which satisfies the specifications.

2. Methodology

In this study the electrochemical bath was prepared using reagents with high grade analytical purity and deionised water. The electrochemical bath used in alloy electroplating Co-W-P consisted of the reagents described in Table 1. The pH of the bath was adjusted by adding ammonium hydroxide (NH_4OH) and sulphuric acid. The substrate used was a rectangular copper plate of surface area 8 cm^2, which was initially polished with sandpaper of 400, 600 and 1200 mesh, treated chemically by immersing in 10% NaOH solution to remove any residual alkali, and the surface activated in 1% H_2SO_4.

Table 1. Electrolytic bath composition

Reagents	**Concentration**
Cobalt sulphate ($COSO_4$)	0.1 M
Saccharin ($C_7H_5NO_3S$)	2.5 g/L
Trisodium citrate ($Na_3C_6H_5O_7$)	0.2 M
Sodium hypophosphite ($NaPO_2H_2$)	0.05M
Sodium tungstate (Na_2O_4W)	0.01M

The electrodeposition was conducted in a galvanostat device, which rotated the rectangular substrate of copper, which operated as the cathode, and inserted it into a cylindrical platinum electrode (the anode). All electrochemical measurements were carried out with a Microquimica-MQPG-01 electrochemical system. The electrodeposition was performed using the operating parameters described in Figure 1. The bath temperature was maintained at 23°C ± 2°C.

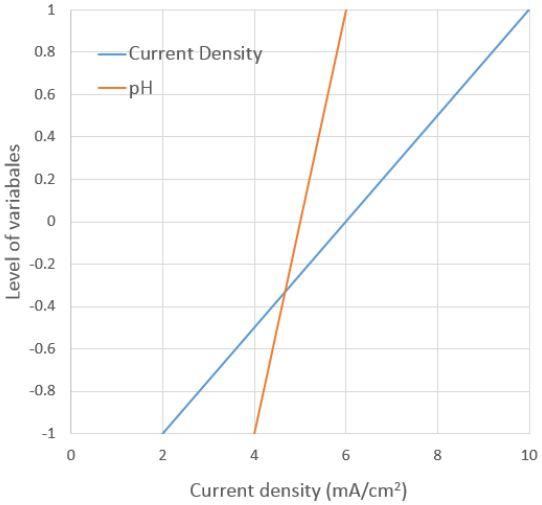

Figure 1. Density and pH variables

A schematic of the experimental setup for the platinum electrodeposition on titanium is shown in Figure 2. The galvanostat device ran at 20 V and 400 mA in a rectangular flow channel with a potentiostat to control the electrode cell. Electrochemical corrosion was measured in a conventional three-electrode cell. The linear potentiodynamic polarisation technique was used to measure corrosion resistance. High current potentiostat/galvanostat PGSTAT 30 was used to feed data to the computer. The working electrode was the copper coated substrate alloy Co-W-P, the reference electrode was a saturated calomel, and the counter electrode was a platinum spiral wire. All the electrochemical corrosion tests were performed in a corrosive medium containing 3.5% NaCl solution at approximately 23°C ambient temperature.

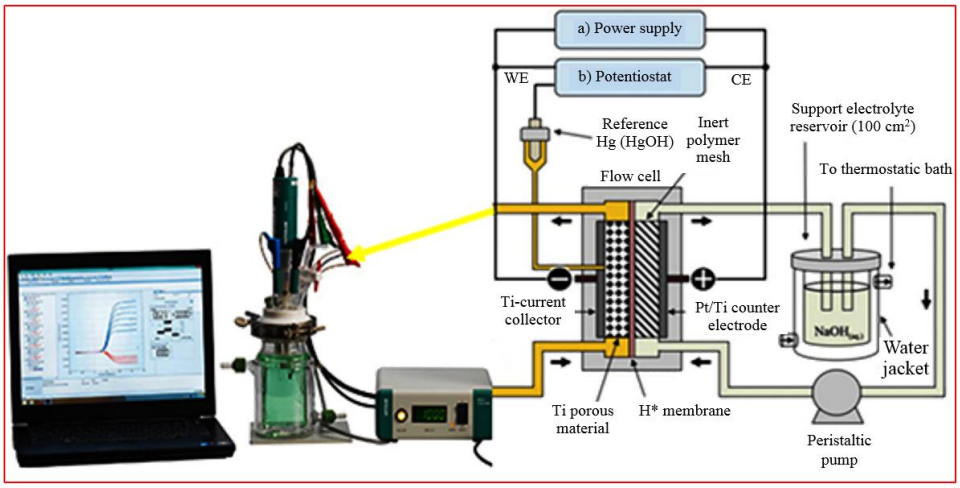

Figure 2. Schematic of the experimental setup for platinum electrodeposition on titanium

The morphology and coating microstructure were analyzed by X-ray fluorescence with a Shimadzu EDX-720 spectrometer. A scanning electron microscope, VEGA- 3SBH, was used to examine the metal coating structure and the thickness of the surface. With this test, the morphology of the deposits and the appearance of cracks and nodules on the surface was explored. In an electroplating process, it is expected that the applied current is used entirely for the deposition of material. As the reactions occur in parallel with metal deposition, i.e. the reduction of hydrogen, in this way, it is difficult to achieve 100% efficiency. The current efficiency (CE) is the ratio of the electrochemical equivalent current density for a specific reaction to the total applied current density. Current efficiency describes the efficiency with which charge (electrons) is transferred within a system, facilitating an electrochemical reaction. The efficiency is calculated according to following equation:

$$CE = \frac{w \times F}{I \times t} \sum \frac{c_i n_i}{M_i} \times 100, \quad (1)$$

where w is the measured mass of the deposit (g), which is the difference between the substrate before and after electrodeposition; t is the deposition time (s); I is applied current (A); n_i is the number of electrons transferred from each metal atom; M_i is the mass of the atomic elements ($gmol^{-1}$); and F is the Faraday constant (96.49 $CMol^{-1}$).

In the experiment, response surface methodology (MSR) was used to analyse the influence of the independent variables in the variable responses. The plan was to check how the corrosion resistance reacted in the interaction of two factors, current and pH density, and also to communicate between lower (-1), upper (1) and centre (0) levels. Figure 3 shows the ionisation and deposition of the test specimens in potentiostatic mode with a steel substrate.

Figure 3(a) shows a non-uniform surface with many cracks that occurred due to internal tension caused by the high content of cobalt. Figure 3(b) shows a more uniform coating with the appearance of small nodules. These appeared because the amount of cobalt decreased progressively. The presence of cracks on the surface of the alloys shows a progressive corrosion resistance of the substance that changes gradually from Figure 3(a) to 3(b), given high resistivity.

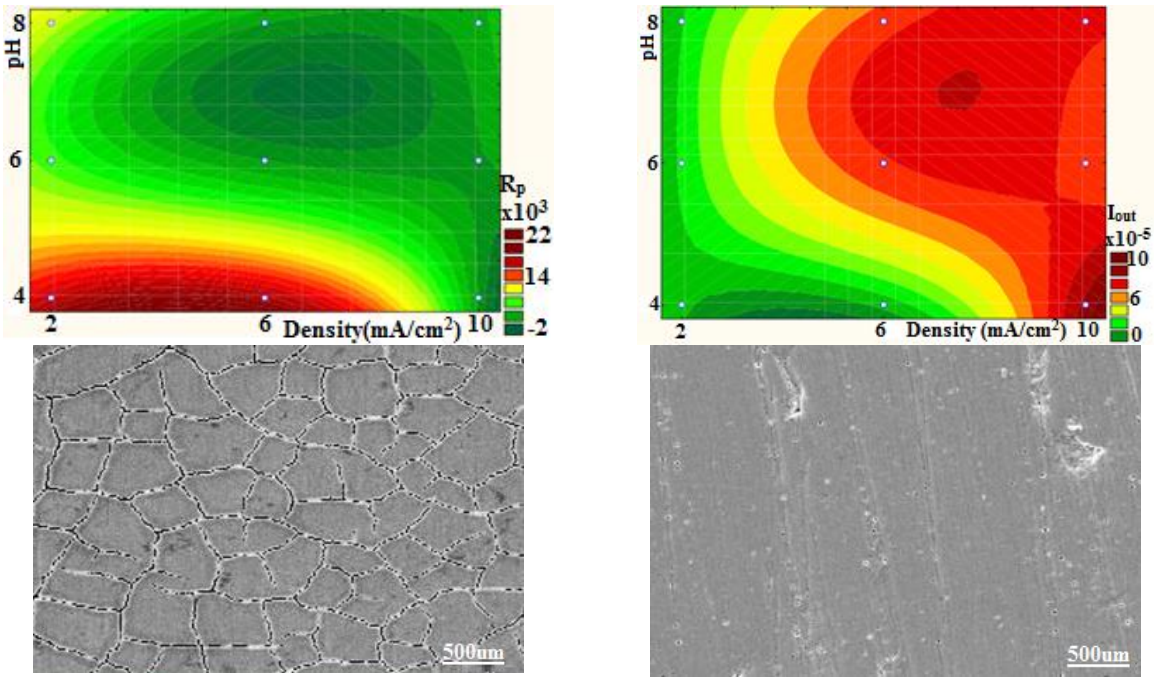

(a) (b)

Figure 3. Corrosion resistance under the influence of current density chain and pH (a) rough surface finishing, (b) good surface finishing

According to the dimensional and geometrical product specifications and verification ISO 4287, the profile parameters were extracted for the Co-W-P alloy. Analysis of the electrochemical measurements took approximately 2.2 hours, long enough to get a stable potential to run the measurements for a smooth surface. The Gaussian filter was set to 0.8 mm; the mean width of the roughness profile elements (RSm) fixed at 1.18 mm; and the root-mean-square slope of the roughness profile (RΔq) was 77.2°. The peak parameters of the roughness profile with the root-mean-square slope of the roughness profile (Rdq) was 86.1° at a Gaussian filter of 2.5 mm with peak count on the roughness profile (RPc) of 0.637 L/mm at +/-0.5 GL.

3. Results and discussion

The results were submitted to non-linear regression analysis to obtain multiple degrees of each parameter. Estimates of coefficients with levels higher than 95% ($P < 0.05$) were included in the highlighted model [17]. The polarisation resistance (Rp) was represented in the form of the independent function factors of a mathematical second order model. The analysis of variance data justified the use of a second order model for the statistical study. Table 2 shows the statistical evaluation determined by the Fisher test for analysis of variance. R^2 was set at 0.98.

Table 2. Analysis of variance for corrosion resistance

Sources	Sum Quadrate	Degree in Liberty	Average Quadrate	F	P
(1)j L+Q	1.2×10^{8}	2	6.1×10^{7}	2.5×10^{4}	0.004
(2) pH L+Q	1.67×10^{7}	2	8.67×10^{7}	3.67×10^{4}	0.003
Interaction between 1 and 2	1.09×10^{8}	4	2.69×10^{7}	1.1×10^{4}	0.007
Residual error	2.4×10^{8}	1	2.37×10^{7}		
Total sum	4.0×10^{8}	9			

An complexing agent, sodium citrate, was added to the electrodeposited Co-W-P alloy. The appropriate concentration of sodium citrate in the bath improved the solubility of metal ions and the buffering ability of the bath, consequently giving a deposit with greater adhesion and gloss. The effect of current density was explored in the range 2 mA/cm² to 10 mA/cm². This current density range was chosen after preliminary tests that observed densities higher than 10 mA/cm³ and less than 70 mA/cm^2, which showed only traces of tungsten in the coating. The analysis of the experimental regression data in the group study showed, with a 95% confidence level, that density was a significant variable in the process of electrodeposition.

3.1. Composition and surface morphology

Table 3 shows the trend in the cobalt sulphate concentration based on the EDX results. With a significant cobalt sulphate concentration, there was a decreasing trend in the content of phosphorus atoms and a small increase in the tungsten atom. This deposition was induced, and phosphorus and tungsten elements were deposited at inverse rates. When more phosphorus was deposited less tungsten was, and vice versa. The best cathode efficiency in the experiment was shown with lower current corrosion and higher polarisation resistance.
Table 3 shows the corrosion resistance results, polarisation resistance and current corrosion for optimisation of the operating parameters Co-alloy and W-P. Each experimental pattern had a total of 8 experiments.

Table 3. Chemical composition and levels of polarisation resistance for current corrosion of Co-W alloy obtained by EDX

j(mA/cm^2)	pH	Co (wght%)	W (wght%)	P (wght%)	E (V)	R_p (Ohm)	I(A)
-1(2)	-1(4.0)	74.2	2.6	22.5	-0.27	16951.00	2.2×10^{-7}
-1(2)	0(6.0)	93.9	1.2	5.0	-0.66	5445.10	1.2×10^{-6}
-1(2)	1(8.0)	92.0	3.2	5.0	-0.67	7751.00	8.90×10^{-7}
0(6)	-1(4.0)	83.0	1.1	15.8	-0.37	18182.00	3.40×10^{-7}
0(6)	0(6.0)	92.0	3.0	5.2	-0.93	1004.20	4.30×10^{-6}
1(10)	-1(4.0)	91.6	1.2	7.1	-0.90	974.50	9.24×10^{-6}
1(10)	0(6.0)	91.0	3.4	5.9	-0.80	910.80	6.2×10^{-6}
1(10)	1(8.0)	90.4	3.9	5.9	-0.77	1718.80	7.60×10^{-6}

Figure 4 shows the behaviours of current density versus pH level. The best corrosion resistance was found when the pH level decreased. With a current density between 2 and 6 mA/cm², higher strength values were obtained. Figure 4(a) shows the extracted profile based on ISO 4287 standard with the amplitude parameter roughness profile of the Gaussian filter at 0.8 mm. Figure 4(b) shows the roughness and waviness profile of a sample cut-off at 2.50 mm. The maximum peak height of the roughness profile is 0.998 GL, and the maximum valley depth of the roughness profile of 1.02 GL, giving the maximum height of the roughness profile. Figure 4(c) shows the nanoparticle segmentation of the surface for the t^2

method of identifying electrodeposition. Figure 4(d) shows a 3D surface view of the corroded part of the electrodeposition at 240 GL.

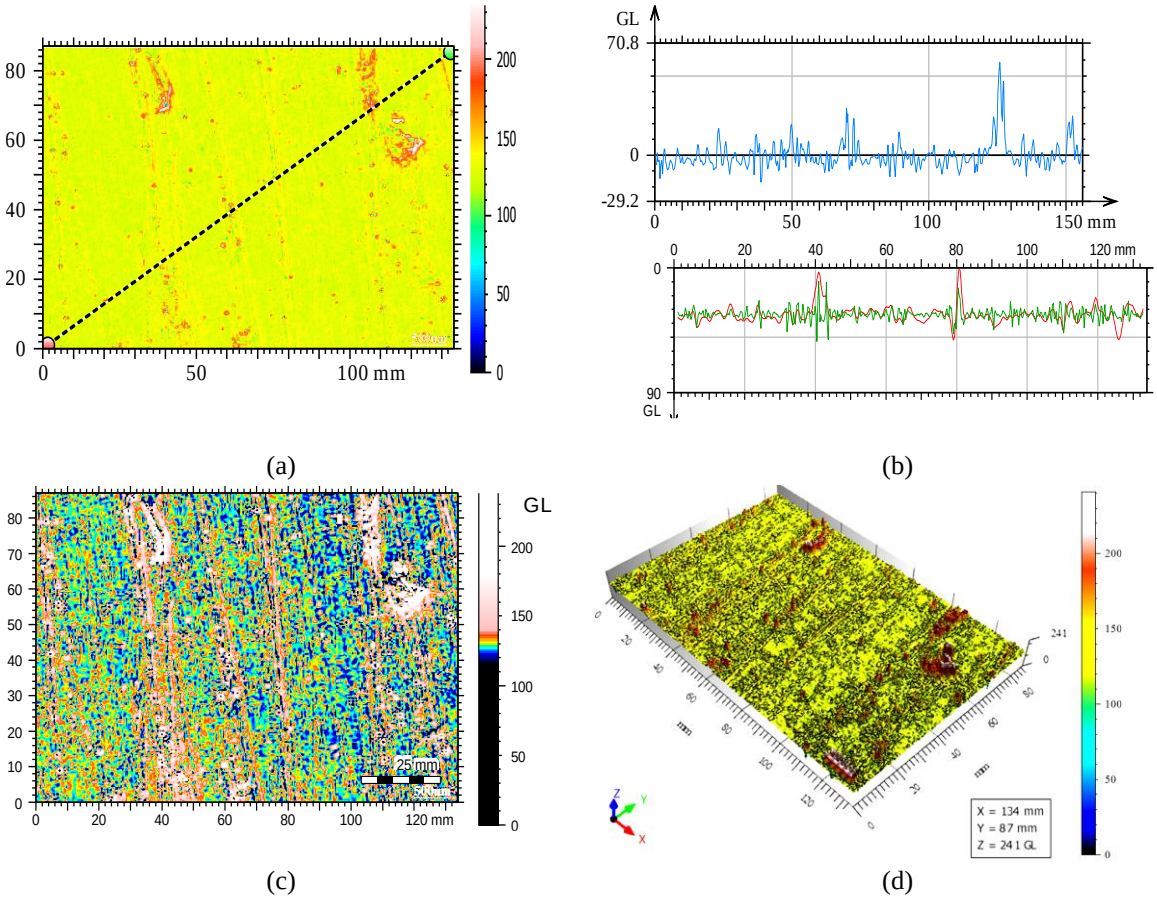

Figure 4. Co-W-P electrodeposited composite coatings, (a) filtered extracted profile, (b) roughness and waviness profile, (c) nanoparticle segmentation of surface, (d) 3D surface view of the corroded part

Figure 5 shows the average power spectrum density (PSD) of the luminance conversion of the fine Co-W-P alloy. The zoom factor was x4 for the non-smoothing parameter value with a wave length of 20.0 mm, amplitude of 0.447 GL, dominant wave length 2.08 mm and maximum amplitude of 52.7 mm, as shown in Figure 5(a). Figure 5(b) shows the morphological envelope method of PSD for the fine Co-W-P alloy with a zoom factor of x4 and a non-smoothing effect spectrum of density to wavelength. The amplitude was 1.21 GL, wavelength 10.9 mm, dominant wavelength 20.1 mm and maximum amplitude 4.93 GL, with spatial frequency 0.0839 mm^{-1} and fractal dimension 2.35. Figure 5(c) shows a zoom factor x4 for PSD and a tolerance limit of 0.75 GL, which is a good tolerance for a Gaussian filter of 0.8 mm profile roughness, amplitude 3787 GL^2, dominant spatial frequency of 0.942mm^{-1} and maximum amplitude of 4742 GL^2, giving a resultant slope of 0.646 of R^2 for an equation of 1.00.

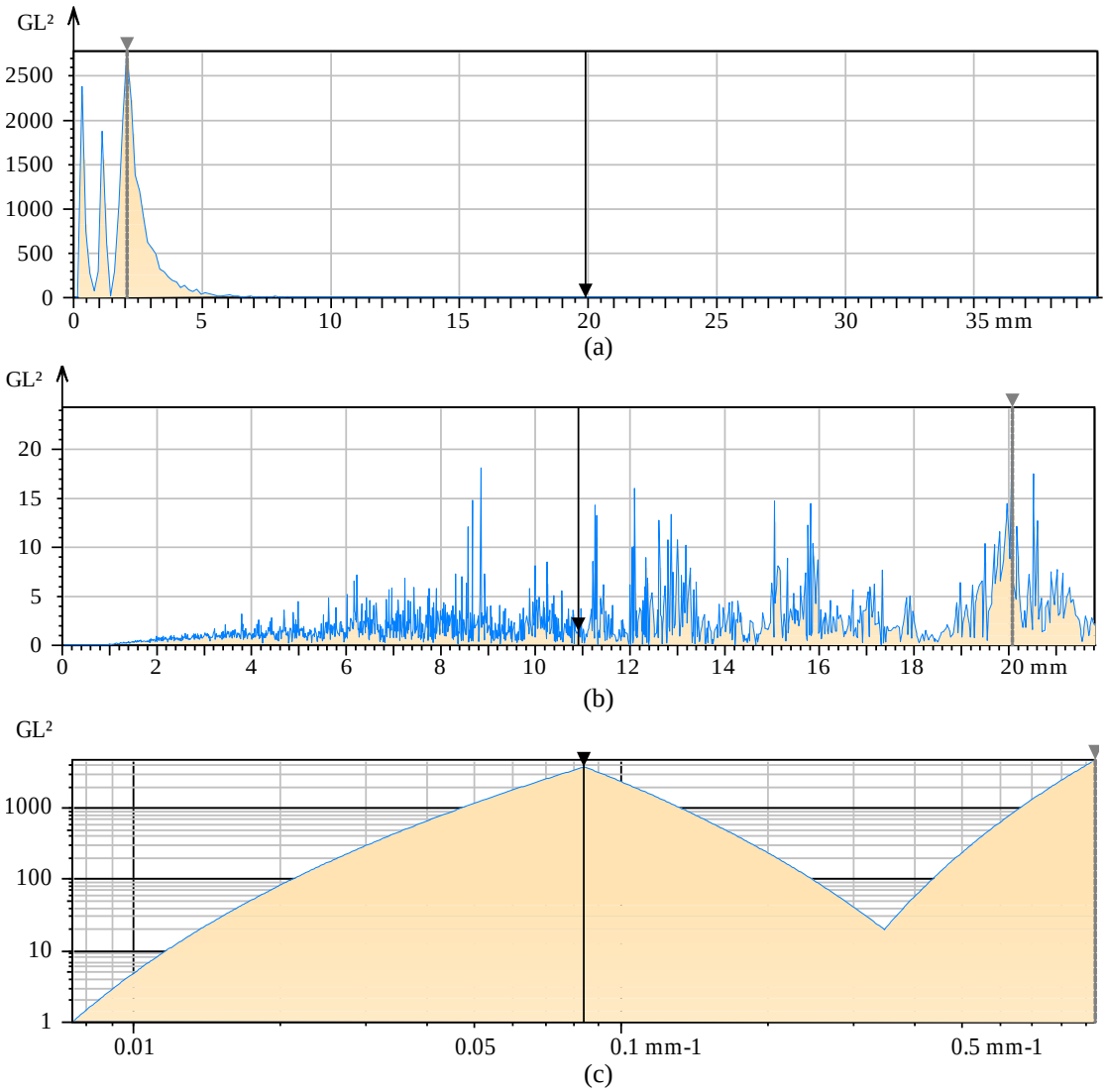

Figure 5. PSD of luminance conversion of the fine Co-W-P alloy, (a) wavelength area, (b) dominant wavelength h, (c) spatial frequency 0.0839 mm^{-1}

4. Conclusions

In this research, a novel coating showed good adhesion and a gloss finish, and a layer with more substantial corrosion resistance with a chemical composition of 1.2% tungsten content, 83.1% cobalt content and 15.7% phosphorus content. Surface methodology and response were used as optimisation tools for enhancing Co-W-P alloy electroplating. A new bath method without complexing agents was used. An unstable process was achieved and good quality Co-W-P alloy films were discovered using an electrochemical bath with a complexing agent, with a lower corrosion resistance coating, showing a chemical composition of 3.3% tungsten content, 90.9% cobalt content and 5.8%. phosphorus content. The addition of tungsten increasingly improved the corrosion resistance of the content, and affected the degree of crystallinity. It was shown that the corrosion resistance increased due to the formation of a dense tungsten oxide film on the surface of the material. A density in the lower level 2 of 6 mA/cm² and acidity of 4.0 pH was identified as best for electrodeposition of Co-W-P. Further study of the same method, using the same composition, could be carried out in future research to allow for both film and nanostructure electrodeposition. Electrodeposition by the potential pulse mode could be used to deposit nanotubes or nanowires using the same method.

References

[1] X. Zhang, B. Li, H.X. Liu , G.H. Zhao, Q.L. Yang, X.M. Cheng, C.H. Wong, Y.M. Zhang, C.W.J. Lim, Atomic simulation of melting and surface segregation of ternary Fe-Ni-Cr nanoparticles. Applied surface science, 465 (2019) 871–879

[2] A.M. Fernandez, J.A. Turner, B. Lara-Lara, T.G. Deutsch, Influence of support electrolytic in the electrodeposition of CueGaeSe thin films, Superlattices and microstructures, 101 (2017) 373-383

[3] P. Jackson, D. Hariskos, E. Lotter, S. Paetel, R. Wuerz, R. Menner, W. Wischmann, M. Powalla, New world record efficiency for Cu (In,Ga) Se2 thin-film solar cells beyond 20%, Progress in photovoltaics: research and Applications, 19 (7) (2011) 894–897.

[4] M. F. de Carvalho, I. A. Carlos. Microstructural characterization of Cu-Sn-Zn electrodeposits produced potentiostatically from acid baths based on trisodium nitrilotriacetic, Journal of electroanalytical chemistry, 823 (2018) 737–746.

[5] B.I. Oladapo, S.A. Zahedi, F. Vahidnia, O.M. Ikumapayi, M.U. Farooq, Three-dimensional finite element analysis of a porcelain crowned tooth, Beni-Suef university journal of basic and applied sciences (2018), https://doi.org/10.1016/j.bjbas.2018.04.002.

[6] B.I. Oladapoa, S.A. Zahedi, S.C. Chaluvadi, S.S. Bollapalli, M. Ismail, Model design of a superconducting quantum interference device of magnetic field sensors for magnetocardiography, Biomedical signal process Control, 46 (2018)116-120

[7] Wan-Shan Kang, Wei-Chen Chou, Wen-Jin Li, Tsung-Han Shen, Chao-Sung Lin, Electrodeposition of Bi2Te3-based p and n-type ternary thermoelectric compounds in chloride baths, Thin Solid Films, 660 (2018) 108–119.

[8] H. Cesiulis, X. Xie, E. Podlaha-murphy, Electrodeposition of Co-W Alloys with P and Ni, Materials science, 15 (2009) 115- 122

[9] S.A. Zahedi, M. Demiral, A. Roy, V.V. Silberschmidt, FE/SPH modelling of orthogonal micro-machining of fcc single crystal, Computational materials science, 78 (2013) 104-109

[10] S.A. Zahedi, A. Roy, V.V. Silberschmidt, Modeling of micro-machining single-crystal fcc metals, Procedia CIRP, 8 (2013) 346-350

[11] Y. Shacham-Diamand, Y. Sverdlov, N. Petrov, Electroless deposition of thin-film Cobalt-Tungsten-Phosphorus layers using tungsten phosphoric acid (H 3[P(W3O10)4]) for ULSI and MEMS applications, Journal of the electrochemical society, 148 (3) (2001) 162-167.

[12] B. I. Oladapoa, A.O.M. Adeoyeb, M. Ismail, Analytical optimization of a nanoparticle of microstructural fused deposition of resins for additive manufacturing, Composites Part B 150 (2018) 248–254

[13] W.F. Hu, H.K.Yuan, H. Chen, G.Z. Wang, G.L. Zhang, Structural and magnetic properties of CoPt clusters, Physic letter A, 378 (2014) 198-206.

[14] S.V. Komogortsev, N.A. Chizhik, E.Yu Filatov, S.V. Korenev, YuV. Shubin, D.A. Verikanov, R.S. Iskhakov, G.Yu Yurkin, Magnetic properties and L10 phase formation in CoPt nanoparticles, Solid State Phenom. 190 (2012) 159-162

[15] L. Favre, V. Dupuis, E. Bernstein, P. Melinon, A. Perez, S. Stanescu, T. Epicier, J. P. Simon, D. Babonneau, J.M. Tonnerre, J.L. Hodeau, Structural and magnetic properties of CoPt mixed clusters, Physic Review B, 74 (2006) 014439

[16] X. Zhang, B. Li, H.X. Liu , G.H. Zhao, Q.L. Yang, X.M. Cheng, C.H. Wong, Y.M. Zhang, C.W.J. Lim. Atomic simulation of melting and surface segregation of ternary Fe-Ni-Cr nanoparticles. Applied Surface Science, 465 (2019) 871–879

[17] Kuang-Hsiang Liao, Cherng-Yuh Su, Yu-Ting Ding, Cheng-Tang Pan, Microstructural revolution of CIGS thin film using CuInGa ternary target during sputtering process, Applied Surface Science, 263 (2012) 476–480